

Prediction of In Vitro Dissolution Profile Using Artificial Neural Networks

Mohamed Azouz Mrad, Kristóf Csorba ¹
Dorián László Galata, Zsombor Kristóf Nagy, Brigitta Nagy ²

¹*Department of Automation and Applied Informatics*

²*Department of Organic Chemistry and Technology
Budapest University of Technology and Economics*

Abstract. In pharmaceutical industry, dissolution testing is part of the target product quality that are essentials in the approval of new products. The prediction of the dissolution profile based on spectroscopic data is an alternative to the current destructive and time-consuming method. Raman and near infrared (NIR) spectroscopies are two complementary methods, that provide information on the physical and chemical properties of the tablets and can help in predicting their dissolution profiles. This work aims to use the information collected by these methods by creating an artificial neural network model that can predict the dissolution profiles of the scanned tablets. Mathematical dissolution models were used to describe the dissolution profiles, some models were compared and evaluated in this work. The ANN models created used the spectroscopies data along with the measured compression curves as an input to predict the dissolution profiles and the mathematical models parameters. It was found that ANN models were able to predict the dissolution profile within the acceptance limit of the f_1 and f_2 factors.

Keywords: Artificial neural networks; Dissolution prediction; Raman spectroscopy; NIR spectroscopy; Mathematical Dissolution models

1 Introduction

In pharmaceutical industry, a target product quality profile is a term used for the quality characteristics that a drug product should process in order to satisfy the promised benefit from the usage and are essentials in the approval of new products or the post-approval changes. A target product quality profile would include different important characteristics, very often one of these is the in vitro (taking place outside of the body) dissolution profile [1]. A dissolution profile represents the concentration rate at which capsules, and tablets emit their drugs into bloodstream over the time. It is especially important in case of tablets that yield a controlled release into the bloodstream over several hours. That offers many advantages over immediate release drugs like reducing the side effects due to the reduced peak dosage and better therapeutic results due to the balanced drug release [2]. In vitro dissolution testing has been a subject of scientific researches for several years and became a vital tool for accessing

product quality performance [3]. However, this method is destructive since it requires immersing the tablets in a solution simulating the human body and time-consuming as the measurements usually take several hours. As a result, the tablets measured represent only a small amount of the tablets produced, also called batch. Therefore, there is a need to find different methods that do not have the limitations of the in vitro dissolution testing. The prediction of the dissolution profile based on spectroscopic data is an alternative on which many articles have been published and showed promising results. Raman and near-infrared (NIR) spectroscopies are two complementary methods that are applied in the pharmaceutical industry. They offer the opportunity to obtain information on the physical and chemical properties of the tablets that can help predicting their dissolution profiles in few minutes without destroying them. Hence, Raman and NIR are recognized as a straight-forward, cost effective alternatives and non-destructive tools in the quality control process [4] [5]. However, these spectroscopies produce a large amount of data as they consist of measurements of hundreds of wavelengths. This data can be filtered out or maintained depending on how much useful information can be extracted from it. This can be achieved using multivariate data analysis techniques such as Principal Component Analysis (PCA).

Several researchers have used the spectroscopies data along with the multivariate data analysis techniques in order to predict the dissolution profiles. Zannikos et al. worked on a model that permits hundreds of NIR wavelengths to be used in the determination of the dissolution rate [6]. Donoso et al. used the NIR reflectance spectroscopy to measure the percentage drug dissolution from a series of tablets compacted at different compressional forces using linear regression, nonlinear regression and partial least square (PLS) models [7]. Freitas et al. created a PLS calibration model to predict drug dissolution profiles at different time intervals and for media with different pH using NIR reflectance spectra [8]. Hernandez et al. used PCA to study the sources of variation in NIR spectra and a PLS-2 model to predict the dissolution on tablets subjected to different levels of strain [9].

Artificial neural networks (ANNs) are very suitable for complex and highly non-linear problems and have been used in pharmaceutical industry in many aspects, such as the prediction of chemical kinetics [10], monitoring a pharmaceutical freeze-drying process [11], solubility prediction of drugs [12]. ANN models have been also used for the prediction of the dissolution profile based on spectroscopic data. Ebube et al. trained an ANN model with the theoretical composition of the tablets to predict their dissolution profile [13]. Galata et al. developed a PLS model to predict the contained drotaverine (DR) and the hydroxypropyl methylcellulose (HPMC) content of the tablets which are respectively the drug itself and a jelling material that slows down the dissolution, based on both Raman and NIR Spectra, and used the predicted values along with the measured compression force as input to an ANN model in order to predict the dissolution profiles of the tablets defined in 53 time points [14]. Using NIR and Raman spectra to predict the DR and HPMC content of the tablets then along with the concentration force predicting the dissolution profile is a fast method that

require minimal amount of human labor and which makes it easier to evaluate a larger amount of the batch. However, using predicted values as input to the ANN model might limit the accuracy of the dissolution profile prediction. Furthermore, training a neural network model to map three inputs to the 53 time points of the dissolution profile, is still a heavy task that might also affect the accuracy of the prediction. Thus, our goal was to create ANN models using different approaches and compare them to the current results. Several mathematical models have been developed for the analysis and the fitting of the drug dissolution data, most of which are presented as nonlinear equations. These models provide a convenient way to describe all the time points of an in vitro dissolution profile using few parameters and a mathematical equation. Our aim was to compare these mathematical models in order to select a suitable model to fit our dissolution data. Extract the useful information directly from the NIR and RAMAN spectra using a multivariate data analysis technique. This information, along with the compression curve of the tablets was used as input of an ANN model created that predicts the parameters of the mathematical model to which the dissolution data is fitted.

2 Data and Methods

In this section, the data used will be described, the methods used for the data pre-processing will be presented as well as the methods used for the dissolution mathematical modeling. The artificial neural networks created will be presented and finally the error measurement methods adopted to evaluate the results.

2.1 Data Description

We have been provided with the measurements of the NIR and RAMAN spectroscopy, along with the pressure curves extracted during the compression of the tablets. The data consists of the NIR reflection and transmission, Raman reflection and transmission spectra, the compression force - time curve and the dissolution profile of 148 tablets. The tablets were produced with a total of 37 different settings. Three parameters were varied: drotaverine content, HPMC content and the compression force. From each setting, four tablets were selected for analysis (37*4). The spectral range for NIR reflection spectra was 4000-10,000 cm^{-1} , with a resolution of 8 cm^{-1} , which represents 1556 wavelength points. NIR transmission spectra were collected in the 4000-15,000 cm^{-1} wavenumber range with 32 cm^{-1} spectral resolution, which represents 714 wavelength points. Raman spectra were recorded in the range of 200-1890 cm^{-1} with 4 cm^{-1} spectral resolution for both transmission and reflection measurements which represents 1691 points. Two spectra were recorded for each tablet in both NIR and Raman. The pressure during the compression of the pill was recorded in 6037 time points. The dissolution profiles of the tablets were recorded using an in vitro dissolution tester. The length of the dissolution run

was 24 h. During this period, samples were taken at 53 time points (at 2, 5, 10, 15, 30, 45 and 60 min, after that once in every 30 min until 1440 min).

2.2 Data Analysis

The collected data were visualized and analyzed using MATLAB and Excel in order to detect and fix missed and wrong values: Setting first point of the dissolution curves to zero, detecting missed values, and fixing negative values found due to error of calibration, etc. Specifically, the data is represented in matrices N_i^n for NIR transmission data and M_j^n for NIR Reflection data, where $i=1556$, $j=714$. R_k^n and Q_k^n respectively for Raman reflection and transmission data where $k=1691$. C_l^n for the compression force data where $l=6037$ and P_s^n for the dissolution profiles where $s=54$. With n representing the number of samples which is equal to 296. All the different NIR, RAMAN and the compression force matrices have been standardized using scikit-learn preprocessing method: StandardScaler. StandardScaler fits the data by computing the mean and standard deviation and then centers the data following the equation $Std(NS) = (NS - u)/s$, where NS is the non-standardized data, u is the mean of the data to be standardized, and s is the standard deviation. All the different standardized NIR, RAMAN and the compression force matrices have been row-wise concatenated to form a new matrix D_m^n where $n=296$ and $m=i+j+2k+l=11686$ as follow: $D_m^n = (N_i^n | M_j^n | R_k^n | Q_k^n | C_l^n)$. After standardization, PCA was applied to the different standardized matrices as well as the merged data D_m^n and in order to reduce the dimension of the data while extracting and maintaining the most useful variations. Basically, taking D_m^n as an example we construct a symmetric $m \times m$ dimensional covariance matrix Σ (where $m=11686$) that stores the pairwise covariances between the different features calculated as follow:

$$\sigma_{j,k} = \frac{1}{n} \sum_{i=1}^n (x_j^{(i)} - \mu_j)(x_k^{(i)} - \mu_k) \quad (1)$$

With μ_j and μ_k are the sample means of features j and k . The eigenvectors of Σ represent the principal components, while the corresponding eigenvalues define their magnitude. The eigenvalues were sorted by decreasing magnitude in order to find the eigenpairs that contains most of the variances. Variance explained ratios represents the variances explained by every principal components (eigenvectors), it is the fraction of an eigenvalue λ_j and the sum of all the eigenvalues. The following plot [Figure 1] shows the variance explained ratios and the cumulative sum of explained variances. It indicates that the first principal components alone accounts for 50% of the variance. The second component account for approximately 20% of the variance. The plot indicates that the seven first principal components combined explain almost 96% of the variance in D . These components are used to create a projection matrix W which we can use to map D to a lower dimensional PCA subspace D' consisting of less features:

$$D = [d_1, d_2, d_3, \dots, d_m], d \in R^m \rightarrow D' = DW, W \in R^{m \times v} \quad (2)$$

$$D' = [d_1, d_2, d_3, \dots, d_m], d \in R^m \quad (3)$$

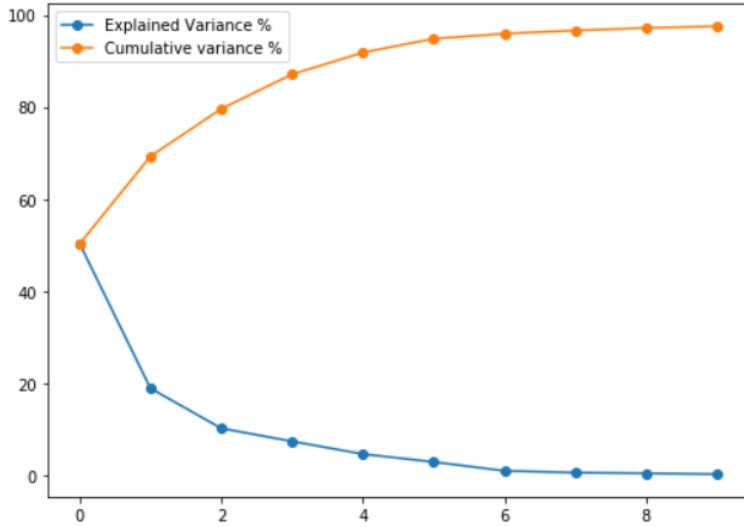


Figure 1: PCA Explained and Cumulative variances

2.3 Curve Fitting

Different mathematical models have been developed for the analysis of drug dissolution data. These dissolution models are described in a paper by Zhang et Al. in which the development of a software program called DDSolver was described [15]. The software contains a model library for fitting dissolution data using a nonlinear optimization method. For this purpose, a wide range of dissolution models were collected. Some of the models that satisfy the criteria of our dissolution profiles and produced pills were chosen: such models do not include parameters that are irrelevant to our dissolution data (based on how the pills were produced) such as a parameter which represents the lag time prior to drug release:

Table 1: Mathematical dissolution models

Model	Equation	Parameters
Weibull 2	$F = 100(1 - e^{-\frac{t^\beta}{\alpha}})$	α, β
Weibull 3	$F = F_{max}(1 - e^{-\frac{t^\beta}{\alpha}})$	$\alpha, \beta, F_{(max)}$
Logistic 1	$F = 100 \frac{e^{\alpha + \beta \cdot \log(t)}}{1 + e^{\alpha + \beta \cdot \log(t)}}$	α, β
Gompertz1	$F = 100e^{-\alpha e^{-\beta \log(t)}}$	α, β
Gompertz 2	$F = F_{max} * e^{-\alpha e^{-\beta \log(t)}}$	$\alpha, \beta, F_{(max)}$

Where in all models F is the fraction (%) of the drug release in time t, and F_{max} is the maximum fraction of drug released at infinite time.

Curve-fit scipy module has been used for the drug dissolution models, it uses non-linear least squares to fit a function, f , to the data by assuming $Dissolution = f(time, *params) + \epsilon$. All the models fitted have been evaluated and compared to each other's based on how well they fit the measured dissolution profiles using a method created that compare the fitted dissolution curves and the measured dissolutions based on the factors f_1 and f_2 that will be described later in details.

2.4 Artificial Neural networks

ANN models were used to predict the dissolution profiles of the tablets. The models were created using the Python library sklearn. Two types of ANN models were created, NNc and NNp respectively for curve and parametric estimation. The models used the rectified linear unit activation function referred to as ReLU on the hidden layers and the weights on the models were optimized using LBFGS optimizer. The mean-squared error (MSE), was the loss function used by the optimizer in both type of models. The two types used the same inputs, Input₁ and Input₂ each time, which are described later in this paper. However, the training target was the 53 dissolution curve points for NNc and the three parameters of the fitted model for NNp. The number of layers on the models and the number of neurons were optimized based on their performances. Regularization term has been varied in order to reduce overfitting. In each training, 16% of the training samples (49 samples) were selected randomly for testing. Accuracy of NNc predictions was calculated by evaluating the similarity of the predicted and measured dissolution profiles using the f_2 and the f_1 values. However, for NNp, the dissolution curves were first reproduced using the predicted parameters and then compared to the measured ones using the same factors.

2.5 Error measurement

Two mathematical methods are described in the literature to compare dissolution profiles [16]. A difference factor f_1 which is the sum of the absolute values of the vertical distances between the test and reference mean values at each dissolution time point, expressed as a percentage of the sum of the mean fractions released from the reference at each time point. This difference factor f_1 is zero when the mean profiles are identical and increases as the difference between the mean profiles increases.

$$f_1 = \frac{\sum_{t=1}^n |R_t - T_t|}{\sum_{t=1}^n |R_t|} * 100 \quad (4)$$

Where R_t and T_t are the reference and test dissolution values at time t .

The other mathematical method is the similarity function known as the f_2 measure, it performs a logarithmic transformation of the squared vertical distances between the measured and the predicted values at each time point. The value of f_2 is 100 when the test and reference mean profiles are identical and decreases

as the similarity decreases.

$$f_2 = 50 \log_{10} \left[\left(1 + \frac{1}{n} \sum_{t=1}^n (R_t - T_t)^2 \right)^{-0.5} \right] * 100 \quad (5)$$

Values of f_1 between zero and 15 and of f_2 between 50 and 100 ensure the equivalence of the two dissolution profiles. The two methods are accepted by the FDA (U.S. Food and Drug Administration) for dissolution profile comparison, however the f_2 equation is preferred, thus in this paper maximizing the f_2 will be prioritized. The average of f_1 and f_2 on the different samples was then calculated and returned.

3 Results and discussions

In this section the results after the PCA decompositions will be discussed. The results of the different mathematical dissolution models and the performance of the Artificial Neural Network models created will be presented.

3.1 Dimensionality reduction using PCA

Principal component analysis transformation was applied in a first step to the standardized NIR and Raman spectra recorded in reflection and transmission mode (N_i^n , M_j^n , R_k^n , Q_k^n matrices) and the standardized compression force curve C_l^n , and in a second step on all the data merged in matrix D_m^n in order to investigate the effect of the transformation on the merged and the separate data. The resulting PCA decompositions, showed that in the case of NIR reflection,

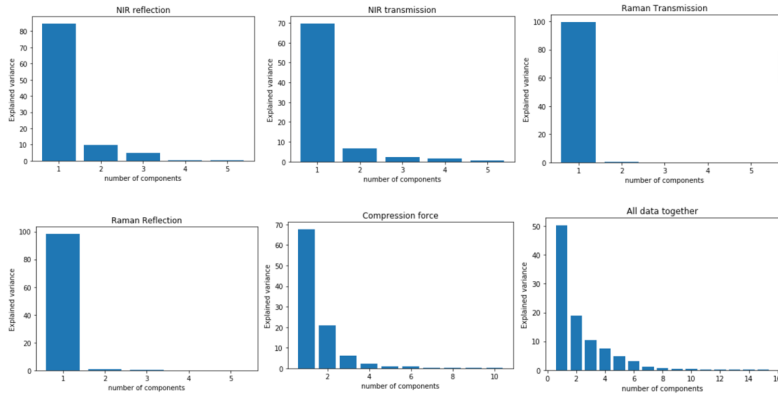


Figure 2: Explained variance of spectral data, compression force, and all merged

three principal components explaining 84.79%, 9.67% and 4.83% of the total variance in the data, respectively, leading to a cumulative explained variance of more than 99%. Four principal components explained more than 80% of the total variances of the NIR transmission data and 95% of the compression force

data. However, for Raman transmission, the first principal component alone explains 99.69% of the variance in the data. The first two principal components explain 98.51% and 1.01% of the variance in the Raman Reflection data, respectively. For matrix D_m^n , 7 principal components explain more than 95% of the variance and 33 explain more than 99% of the merged standardized data. These data resulting from the PCA decomposition were used as the inputs for the Artificial neural network models. Two different inputs were created for the ANN models. Input₁ was composed of the most important principal components of the different data. All components that explain less than 2% of the variance were eliminated, 12 principal components from the different data remained explaining a total average of 95% of the variance. Input₂ maintain 99% of the variance in the merged data with 33 principal components.

Table 2: Inputs selected for the ANN models

Input name	Composition				
	NIR RE	NIR TR	Raman Tr	Raman Re	Compression
Input ₁	3, 99.3%	3, 78.8%	1, 99.96%	1, 98.51%	4, 96.83%
Input ₂	33 PCs, 99% of the variance of all data merged				

3.2 Dissolution Fitting

The five mathematical models described earlier were fitted to the measured dissolution profiles. These dissolution models were evaluated and compared to each other's based on their average f_1 and f_2 values when compared to the measured dissolution profiles. Results have been sorted in descending order as follow: Results showed that fitting the dissolution profiles to the parametric

Table 3: Fitting accuracy of parametric models

	Model	Average f_1	Average f_2
1	Weibull 3	2.84	78.62
2	Weibull 2	5.25	70.05
3	Logistic 1	5.29	65.50
4	Gompertz 2	6.76	64.88
5	Gompertz 2	10.55	59.41

models caused a significant data loss. The measured dissolution profiles can be reproduced in the best case using Weibull 3 model. However, the other Weibull 2, Logistic and both Gomperts models did not perform as good as the Weibull 3. Further investigations showed that the average f_1 is higher during the first few hours of the dissolution profiles and is decreasing over time. [Figure 3] shows the

cumulative f_1 value over a dissolution run t of the reproduced Weibull 3 curve W and the measured curve M : $f_1(M, W, t)$. The average starts at $f_1(M, W, 1) = 24.33\%$ in the first hour, and the cumulative average decreases to $f_1(M, W, 5) = 7.28\%$ in five hours. The average f_1 keeps decreasing over time from $f_1(M, W, 10) = 4.94\%$ to $f_1(M, W, 20) = 3.1\%$ until it reaches $f_1(M, W, 53) = 2.84\%$ at the end of the dissolution run which correspond to the average f_1 for the Weibull 3 reproduced curve compared to the measured curve. Based on the previous

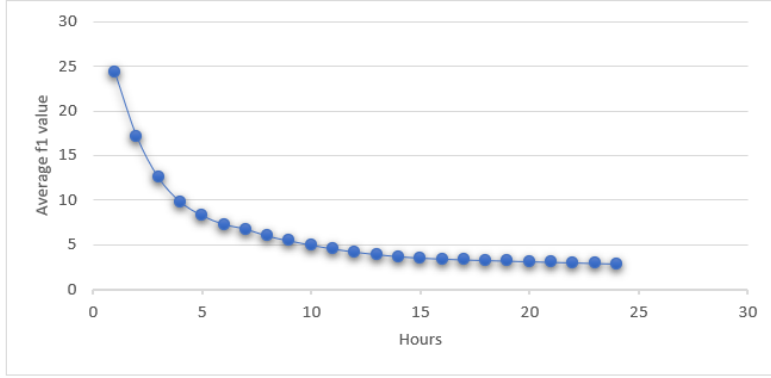


Figure 3: Weibull 3 Cumulative f_1 average over the dissolution run

results, the Weibull 3 model parameters α , β and F_{max} were used as a training target for the neural network models NN_p , as it is the dissolution parametric model that fitted the best the measured dissolution profiles.

3.3 Predicting the Dissolution Profile by Artificial neural network

Four ANN settings were created in total, two in each type (NN_c and NN_p) with the two inputs $Input_1$ and $Input_2$. For each setting, 100 trainings with randomly

Table 4: ANN models

	NN_c (predicting 53 timepoints)	NN_p (predicting 3 parameters)
$Input_1$	Model 1-1	Model 2-1
$Input_2$	Model 1-2	Model 2-2

selected testing datasets were run. The average f_2 of the 100 trainings was recorded. For NN_c models, the number of neurons was increased from one to 13 and results were recorded. A second layer and then a third layer having all the same number of neurons, were added in order to check the effect of deeper network on the behavior of the models and their results. Results showed that increasing the number of neurons until 10 neurons was beneficial and improved

the average f_2 value on both model 1-1 and model 1-2. however, after 10 neurons both models maintained the same behavior and even the results decreased starting from the 12th neurons. Adding further hidden layers, slightly increased the performance of the models starting from 5 neurons when adding a second layer and a third layer on Model 1-1. Adding a second layer on Model 1-2 increased the results after the 5th neurons, while it was only beneficial after the 7th neuron for the third layer. Both models with at least one hidden layer and

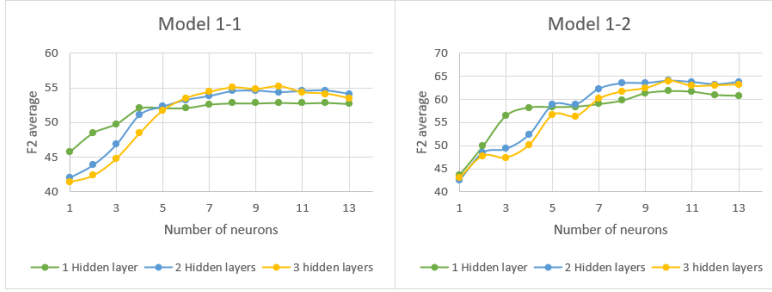


Figure 4: Average f_2 values, using different layers and neuron numbers

7 neurons, were capable to predict all the measured dissolution profile of all the 49 test tablets within the acceptance range of both f_1 and f_2 factors. Adding more neurons and more layers was beneficial in improving the prediction. The best f_2 result achieved for Model 1-1 was by using one hidden layer with 10 neurons. However, the best f_2 result for Model 1-2 was achieved by three layers each having 10 neurons. This might be due to the higher number of features in the input used in Model 1-2 (33 features) compared to only 12 features in Model 1-1 inputs.

Table 5: Results of best performing NNc models

Model	f_2 value of the best ANN model	f_1 value of the best ANN model
Model 1-1	67.05	6.51
Model 1-2	70.35	5.29

The same approach was used on NNp models Model 2-1 and Model 2-2 to investigate the number of neurons and layers to be used and their effect on the behavior of the models. Results were not very promising as for the different settings, the best f_2 average on the 100 trainings was 41.71. This average was achieved by using only one hidden layer with one neuron network.

Increasing the number of neurons and adding further hidden layers to the network, only yielded to smaller f_2 averages. The most performing model had an $f_2 = 50.45$ and $f_1 = 15.45$ on the testset. Only some of the predicted dissolution

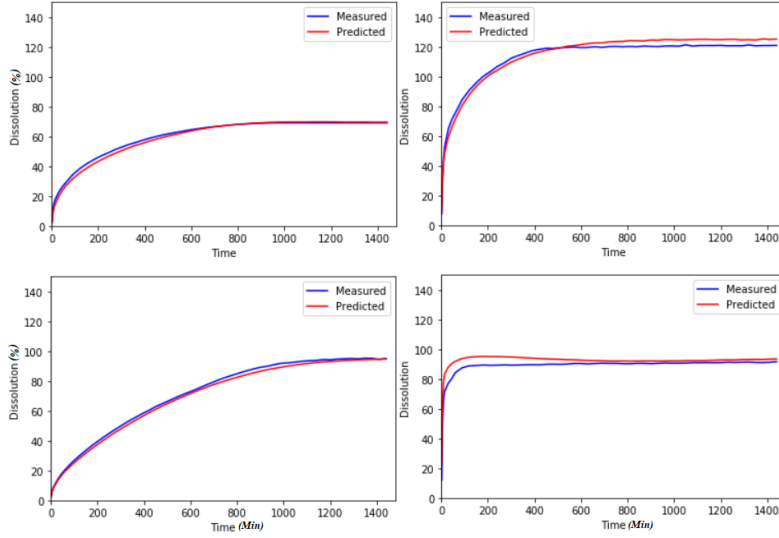
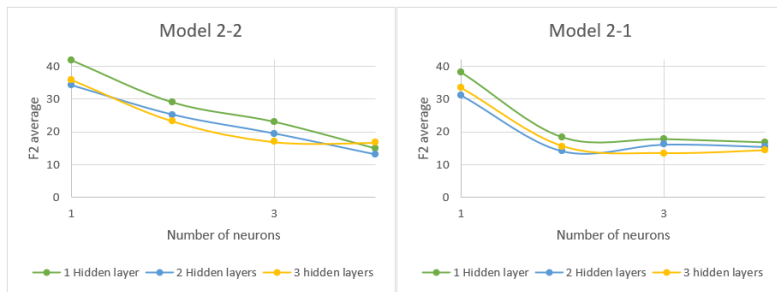


Figure 5: Sample predicted dissolution profiles using Model 1-1

profiles fit the acceptance range of f_1 and f_2 factors. Thus, the predicted dissolution profiles cannot be accepted as equivalent to the measured ones due to the data loss caused by the transition from the numerical to parametric model at first by the fitting then by the ANN prediction. The parametric modeling of the dissolution profiles as well as their prediction using Artificial neural networks require more research.


 Figure 6: Average F_2 values, using different layers and neuron numbers Model 2-2 and 2-1

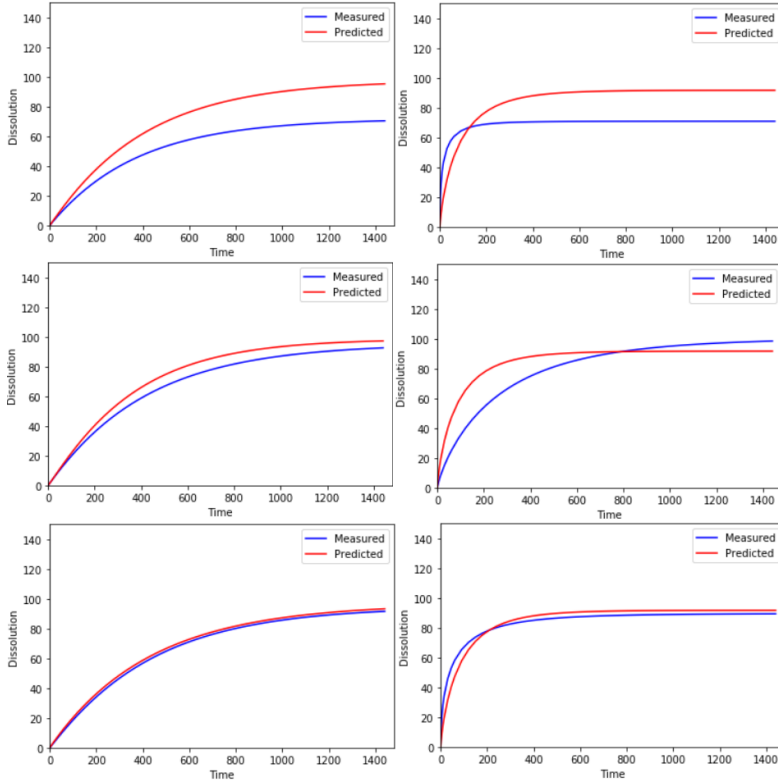


Figure 7: Sample predicted dissolution curves using best performing Model 2-1

4 Conclusion

The current work aimed to utilize the recorded NIR and Raman spectroscopy data along with the compression force to predict the dissolution profiles of tablets produced with 37 different settings. The dimensionality of the data was reduced using PCA, then used as an input for the four different neural models created. ANN models used Limited-memory BFGS as optimizer, and the dissolution profiles and Weibull model parameters as training targets. It was found that ANN models using NIR and Raman spectroscopy along with the compression force, can predict the dissolution profiles withing the acceptance range of the f2 and f1 factors. The results show that the in vitro dissolution testing can be replaced by more advanced methods that use similar data providing a large amount of information about the tablets. However, predicting the mathematical parameters require further research as the ANN models created were not able to predict the parameters of the Weibull model that can reproduce the curves within the acceptance range of f1 and f2.

Acknowledgments

Project no. FIEK_16-1-2016-0007 has been implemented with the support provided from the National Research, Development and Innovation Fund of Hungary, financed under the Centre for Higher Education and Industrial Cooperation Research infrastructure development (FIEK_16) funding scheme.

References

- [1] X. Y. Lawrence, "Pharmaceutical quality by design: product and process development, understanding, and control," *Pharmaceutical research*, vol. 25, no. 4, pp. 781–791, 2008.
- [2] G. A. Susto and S. McLoone, "Slow release drug dissolution profile prediction in pharmaceutical manufacturing: A multivariate and machine learning approach," in *2015 IEEE International Conference on Automation Science and Engineering (CASE)*, pp. 1218–1223, IEEE, 2015.
- [3] R. Patadia, C. Vora, K. Mittal, and R. Mashru, "Dissolution criticality in developing solid oral formulations: from inception to perception," *Critical Reviews in Therapeutic Drug Carrier Systems*, vol. 30, no. 6, 2013.
- [4] A. Hédoux, "Recent developments in the raman and infrared investigations of amorphous pharmaceuticals and protein formulations: a review," *Advanced drug delivery reviews*, vol. 100, pp. 133–146, 2016.
- [5] J. U. Porep, D. R. Kammerer, and R. Carle, "On-line application of near infrared (nir) spectroscopy in food production," *Trends in Food Science & Technology*, vol. 46, no. 2, pp. 211–230, 2015.
- [6] P. N. Zannikos, W.-I. Li, J. K. Drennen, and R. A. Lodder, "Spectrophotometric prediction of the dissolution rate of carbamazepine tablets," *Pharmaceutical research*, vol. 8, no. 8, pp. 974–978, 1991.
- [7] M. Donoso and E. S. Ghaly, "Prediction of drug dissolution from tablets using near-infrared diffuse reflectance spectroscopy as a nondestructive method," *Pharmaceutical development and technology*, vol. 9, no. 3, pp. 247–263, 2005.
- [8] M. P. Freitas, A. Sabadin, L. M. Silva, F. M. Giannotti, D. A. do Couto, E. Tonhi, R. S. Medeiros, G. L. Coco, V. F. Russo, and J. A. Martins, "Prediction of drug dissolution profiles from tablets using nir diffuse reflectance spectroscopy: a rapid and nondestructive method," *Journal of pharmaceutical and biomedical analysis*, vol. 39, no. 1-2, pp. 17–21, 2005.
- [9] E. Hernandez, P. Pawar, G. Keyvan, Y. Wang, N. Velez, G. Callegari, A. Cuitino, B. Michniak-Kohn, F. J. Muzzio, and R. J. Románach, "Prediction of dissolution profiles by non-destructive near infrared spectroscopy

- in tablets subjected to different levels of strain,” *Journal of pharmaceutical and biomedical analysis*, vol. 117, pp. 568–576, 2016.
- [10] M. Szaleniec, M. Witko, R. Tadeusiewicz, and J. Goclon, “Application of artificial neural networks and dft-based parameters for prediction of reaction kinetics of ethylbenzene dehydrogenase,” *Journal of computer-aided molecular design*, vol. 20, no. 3, pp. 145–157, 2006.
- [11] E. N. Drăgoi, S. Curteanu, and D. Fissore, “On the use of artificial neural networks to monitor a pharmaceutical freeze-drying process,” *Drying Technology*, vol. 31, no. 1, pp. 72–81, 2013.
- [12] A. G. JOUYBAN, S. Soltani, and Z. K. ASADPOUR, “Solubility prediction of drugs in supercritical carbon dioxide using artificial neural network,” 2007.
- [13] N. K. Ebube, T. McCall, Y. Chen, and M. C. Meyer, “Relating formulation variables to in vitro dissolution using an artificial neural network,” *Pharmaceutical development and technology*, vol. 2, no. 3, pp. 225–232, 1997.
- [14] D. L. Galata, A. Farkas, Z. Könyves, L. A. Mészáros, E. Szabó, I. Csontos, A. Pálos, G. Marosi, Z. K. Nagy, and B. Nagy, “Fast, spectroscopy-based prediction of in vitro dissolution profile of extended release tablets using artificial neural networks,” *Pharmaceutics*, vol. 11, no. 8, p. 400, 2019.
- [15] Y. Zhang, M. Huo, J. Zhou, A. Zou, W. Li, C. Yao, and S. Xie, “Dd-solver: an add-in program for modeling and comparison of drug dissolution profiles,” *The AAPS journal*, vol. 12, no. 3, pp. 263–271, 2010.
- [16] J. Moore and H. Flanner, “Mathematical comparison of dissolution profiles,” *Pharmaceutical technology*, vol. 20, no. 6, pp. 64–74, 1996.